Lawrence Berkeley National Laboratory
Lawrence Berkeley National Laboratory

Title
Electron beam exposure mechanisms in hydrogen silsesquioxane investigated by vibrational spectroscopy and in-situ electron beam induced desorption

Permalink
https://escholarship.org/uc/item/26z54299

Author
Olynick, D.L.

Publication Date
2010

Peer reviewed

eScholarship.org Powered by the California Digital Library
University of California

Electron beam exposure mechanisms in hydrogen silsesquioxane investigated by vibrational spectroscopy and in-situ electron beam induced desorption.

D.L. Olynick, B. Cord, A. Schipotinin, D.F. Ogletree, P.J. Schuck

[†]*Lawrence Berkeley National Laboratory, Molecular Foundry,*
1 Cyclotron Road, Berkeley CA 94720 USA

Abstract

Hydrogen Silsesquioxane (HSQ) is used as a high-resolution resist with resolution down below 10-nm half-pitch. This material or materials with related functionalities could have widespread impact in nanolithography and nanoscience applications if the exposure mechanism was understood and instabilities controlled. Here we have directly investigated the exposure mechanism using vibrational spectroscopy (both Raman and Fourier transform Infrared) and electron beam desorption spectroscopy (EBDS). In the non-networked HSQ system, silicon atoms sit at the corners of a cubic structure. Each silicon is bonded to a hydrogen atom and bridges 3 oxygen atoms (formula: $HSiO_{3/2}$). For the first time, we have shown, via changes in the Si-H_2 peak at ~2200 cm^{-1} in the Raman spectra and and the release of SiH_x products in EBID, that electron-beam-exposed material crosslinks via a redistribution reaction. In addition, we observe the release of significantly more H_2 than SiH_2 during EBID, which is indicative of additional reaction mechanisms. Additionally, we compare the behavior of HSQ in response to both thermal and electron-beam induced reactions.

electronic mail: dlolynick@lbl.gov

Electron beam exposure mechanisms in hydrogen silsesquioxane investigated by vibrational spectroscopy and in-situ electron beam induced desorption.

D.L. Olynick, B. Cord, A. Schipotinin, D.F. Ogletree, P.J. Schuck

[†] *Lawrence Berkeley National Laboratory, Molecular Foundry,*
1 Cyclotron Road, Berkeley CA 94720 USA

Introduction

As a high-resolution negative-tone electron-beam resist with both high mechanical stability and good etch-resistance properties, hydrogen silsesquioxane (HSQ) has become a material of considerable interest for the nanolithography and nanoscience community. While its first resist applications were with electron beam systems,[1] HSQ has been successfully applied to both EUV[2] and nanoimprint lithographic applications as well.[3-4] Using electron-beam lithography (EBL), 11-nm half-pitch gratings in 70-nm-thick films[5] and sub-10 nm half-pitch gratings in 30-nm-thick films[6] have been fabricated using HSQ, making it one of the highest-resolution electron resists available. Furthermore, compared to carbon-based high-resolution resists, HSQ's SiO_2-like composition results in a significantly higher modulus and less resist collapse, a plaguing issues for dense, high resolution features. This SiO_2-like composition also results in excellent pattern-transfer selectivity to a variety of materials.[4-5,7] The fully-condensed HSQ structure has the formula $(HSiO_{3/2})_n$.[8-9] For $n = 8$, the proposed structure of HSQ is cubic, with silicon and hydrogen atoms at the vertices and oxygen atoms forming the edges. However, spin-on films of HSQ are fabricated by sol-gel polymerization which produces cage- or ladder-like, rather than cubic, structures.[10] Isolated polymers will cross-link during thermal or radiation treatment which results in an increase in the ratio of Si-O to Si-H bonds.[11] To create a lithographic pattern, unexposed regions of HSQ are dissolved away in either aqueous base solutions[12] or a variety of organic solvents,[13] leaving a patterned film on the substrate.

The exact mechanism leading to crosslinking during electron-beam or other high resolution exposure techniques are not well-understood. Based on Fourier transform infrared spectroscopy (FTIR) investigations which showed a loss in Si-H bonds and increase in cross-linking between neighboring HSQ polymers, Namatsu *et al*[1] speculated that crosslinking is achieved in a three-step mechanism. In the first step, Si-H bonds in the film are broken to form radical sites. The radical sites on neighboring cages then become bridged with oxygen in the presence of absorbed water, linking the cages and finally produces water as shown in the following reaction schemes:

$$2HSiO_{3/2} + \text{electron beam} \rightarrow 2Si\bullet + H_2 \quad (1)$$

$$2Si\bullet + 2\ H_20 \rightarrow 2SiOH\ +\ H_2 \quad (2)$$

$$2SiOH \rightarrow 2Si0_{1/2} +\ H_20 \quad (3)$$

However, this proposed electron beam cross-linking mechanism has never been substantiated.

Furthermore, since Namatsu’s initial work, a number of authors have documented various instabilities and irreproducibilities[14-16] when working with HSQ which limits its use as a resist. For instance, HSQ exposure dose is dependent on order in which neighboring areas are expososed .[15] Investigations using scanning transmission x-ray microscopy show that the types of chemical changes induced by electron-beam exposure show an usual dependence on both exposure area and electron dose.[17] These chemical changes are initiated by the beam, and unfortunately can extend well beyond exposed area. These instabilities must be understood and controlled to take advantage of HSQ type materials for production-worthy processes such as EUV lithography or even to expect repeatability in smaller-scale electron beam prototyping.

Here we investigate the complicated exposure mechanisms in HSQ using both electron-beam- and thermally-treated HSQ using Raman spectroscopy, as well as electron beam induced desorption (EBID). Using these complementary techniques, we have confirmed that electron beam cross-linking occurs in part by a redistribution reaction where Si-O-Si linkages result when hydrogen is redistributed to form $Si-H_x$ bonds (x =2-4) EBID lends insight to additional reactions that may be occurring including reactions that produce a silicon rich oxide.

Experiment

FTIR and Raman spectroscopy have proven to be powerful tools in the study of lithographic resist systems and polymer systems in general.[18] The techniques are complementary: Raman scattering is sensitive to modes that result in a change in molecular polarizability upon vibration, while IR spectroscopy is sensitive to modes that result in a change in molecular dipole moment; both are sensitive to, and therefore reporters of, the local environments surrounding the active bonds. However, Raman spectroscopy has a spatial-resolution advantage over FTIR; diffraction-limited spot sizes below 500 nm are readily achievable, compared to 8-10 μm in FTIR. In these experiments, we characterized electron beam exposed materials using Raman spectroscopy and compared to thermally-treated HSQ films investigated with both FTIR (Varian 3200 FTIR spectrometer) and Raman (HeNe wavelength = 632.8 nm, diffraction limited spot verified at ~300 nm) spectroscopy.

Optimum spectroscopy measurements are obtained when the films are on appropriate substrates. Silicon, fused silica, glass, and quartz were all investigated as substrates for HSQ. Figure 1 shows the baseline Raman spectra (no film present) for three of these substrates (fused silica and quartz are similar). Fused silica and quartz tend to offer the lowest overall background for Raman measurements, but silicon is IR-

transparent and thus the better substrate for FTIR. To study the higher-wave-number peaks (beyond about 1100 cm^{-1}) of interest in this work, silicon can be used in both techniques.

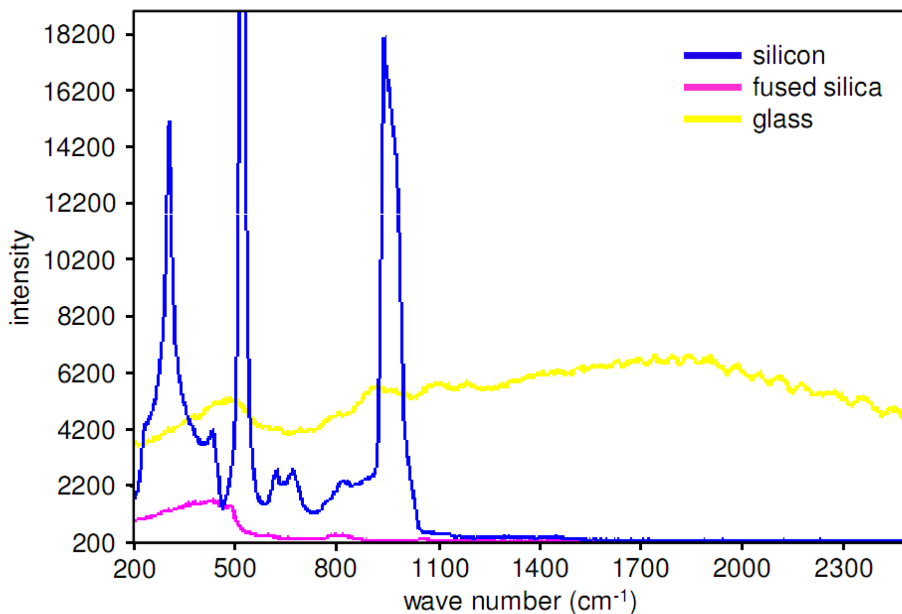

Figure 1: Baseline Raman spectra for silicon, fused silica, and glass substrates. Both silicon and fused silica have minimal baseline signal in the frequency range of interest (~1800-2500 cm^{-1}), although silicon has considerable background signal at lower frequencies. The high broadband background signal of glass, which is likely from autofluorescence due to the presence of more impurities than in fused silica, makes it unsuitable for these experiments. The spectra for quartz was very similar to that of fused silica and is not shown here.

Thermal Behavior

In order to characterize the spectroscopic response to thermal excitation, HSQ films ~ 150 nm thick were spin-coated using 6% solution of HSQ in MIBK (Dow Corning, XR-1541). Films were studied as-spun or heat-treated by baking for one hour at temperatures up to 400°C

Figure 2 shows FTIR and Raman data for HSQ as-spun and thermally treated (100, 200, 300, and 400 °C) on silicon. This result is consistent with previous observations of HSQ baking via FTIR.[19-20] The large peak at ~2256 cm^{-1} is present in both Raman and FTIR and has been identified as the "stretching" vibrational mode of the Si-H bond in HSQ, and decreases substantially with baking temperature. As described in detail in table I, several other modes present in the HSQ are the Si-O-Si large-angle stretching mode at ~1135 cm^{-1}, the HSQ Si-O-Si small-angle stretching mode at ~1075 cm^{-1}, the H-Si-O large angle vibration at 875 cm^{-1} and the O-Si-O bending vibration at ~838^{-1}. From the FTIR data, the ~ 838 cm^{-1}, 875 cm^{-1}, and 1150 cm^{-1} peaks decrease, and the 1070 cm^{-1} peak increases as more Si-O-Si linkages are formed. A very weak mode appears at ~2200 cm^{-1}, corresponding to the stretching mode of the $Si\text{-}H_2$ which arises during heating due to the redistribution reaction:

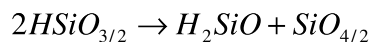

$$2HSiO_{3/2} \rightarrow H_2SiO + SiO_{4/2}$$

n (cm^{-1})	Mode	Change with Increasing Temperature (Raman)	Change with Increasing Temperature (FTIR)
2256	Si-O-Si stretching[21-22]	↓	↓
2200	$Si-H_2$ stretching[10]	↑	↑
1135	Si-O-Si stretching[21-22]	peak not visible	↓
1075	$Si-O_2$ vibrations[22]	Broadening, increase or decrease unclear	↑
990	Associated band to 2200 or SiOH[10]	↑	peak not visible
930	Associated band to 2256[21]	↓	peak not visible
875	O-Si-H bending	↓	↓
838	O-Si-O bending[22]	Broadening, increase or decrease unclear	↓
690	Si-O-Si[21]	Broadening, increase or decrease unclear	peak not visible
581	O-Si-O bending[21]	Broadening, increase or decrease unclear	peak not visible

Table I: Vibrational modes in HSQ that can be observed as peaks in Raman and/or FTIR spectroscopy. The wave number of each peak is listed, as well as the response of each peak (increase, decrease, or broadening) to increased thermal excitation.

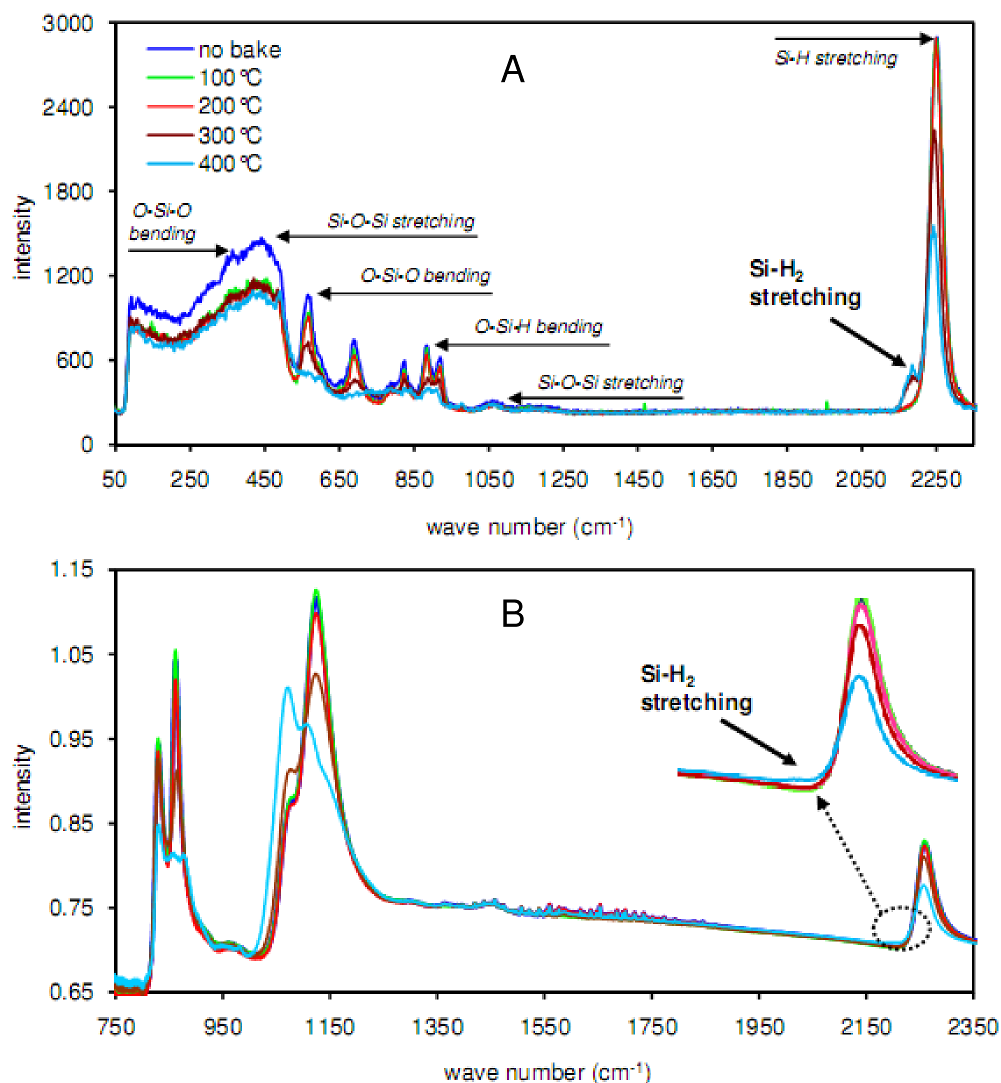

Figure 2: A) Raman spectrum of HSQ on a quartz substrate after 60 minutes of baking at various temperatures. The decrease in the Si-H peak at ~2250 cm^{-1} with increasing temperature is clearly visible, as is the presence of the Si-H$_2$ peak at higher temperatures. B) FTIR spectrum of HSQ on a silicon substrate (normalized to the Si background spectrum) after 60 minutes of baking at several temperatures. The Si-H decrease is visible, but even in the magnified inset it is difficult to see the Si-H$_2$ peak.

Past a certain temperature threshold, higher bake temperatures will cause the Si-H peak to decrease and the Si-H$_2$ peak to increase correspondingly. This shows that, at high temperatures, HSQ will crosslink via a redistribution reaction involving 3 Si atoms; one Si will bond to 2 oxygen atoms and 2 hydrogen atoms,

while the other two will form a bridge across neighboring cages to further network the system, with one of the remaining Si atoms bonded to three oxygen atoms and a hydrogen and the other bonded to four oxygen atoms. This reaction, previously identified during thermal curing of HSQ,[10,22] is illustrated in figure 3. It turns out this reaction also occurs in electron beam exposed material.

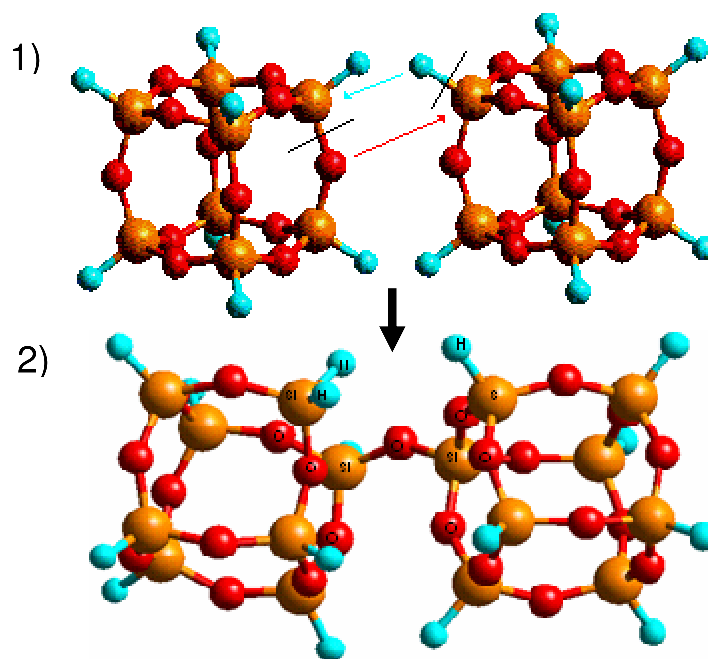

Figure 3: Schematic illustration of the redistribution reaction that may be partially responsible for crosslinking in HSQ. A Si-H and Si-O bond are broken on adjacent HSQ cages (1). The resulting oxygen radical bonds to the site formerly occupied by the hydrogen atom on the adjacent cage, while the now-free hydrogen atom bonds to the Si atom at the site formerly occupied by the oxygen atom, resulting in two slightly altered HSQ cages connected by an oxygen atom (2). Note that this reaction does not depend on the presence of any external reactant, such as water, in order to occur.

Electron-Beam Exposure

Raman studies of HSQ films exposed to various electron doses produced results very similar to the thermal data outlined above. For the e-beam exposure experiments, silicon substrates were coated with HSQ to a thickness of ~150 nm and exposed using a Vistec VB300 EBL tool with a beam energy of 100 KeV (the resist was not prebaked prior to exposure). Patterns consisting of rectangles large enough to be examined in the Raman system were written at various doses, as well as high-dose reference marks to aid pattern location; all Raman measurements were performed on the exposed, undeveloped resist.

As in the case of the thermal measurements, the Raman spectra gave a much more detailed picture of the Si-H and Si-H_2 bond behavior compared to FTIR data. Figure 4 shows the Raman spectra in the frequency range of interest for HSQ exposed at various doses, normalized to the background signal of the silicon substrate. Once again, the Si-H peak at ~2256 cm^{-1} shrinks considerably as a function of electron dose. Unlike the thermal-curing results, both Si-H_2 and Si-H_3 peaks are present. At some doses the individual peaks are difficult to resolve and we instead see a broad band (width of ~50 cm^{-1}) in the 2150-2200 cm^{-1} range, while at other doses (figure 5) two peaks at ~2154 and 2194 cm^{-1} are clearly resolved. The ~2154 cm^{-1} absorption peak corresponds to Si-H_3, which suggests that the redistribution reaction can continue to occur until volatile silane (SiH_4) is produced (SiH_3 is an intermediate product in the production of silane).[22] This is consistent with the observation that, with increasing dose, the Si-H_2 peak decreased while Si-H_3 increased; at the highest examined dose (15 mC/cm^2) the Si-H_2 peak is undetectable. This shows that HSQ crosslinking during electron-beam exposure occurs, at least partially, via redistribution reactions which does not depend on the presence of hydrolyzed bonds as in the Namatsu-proposed mechanism.

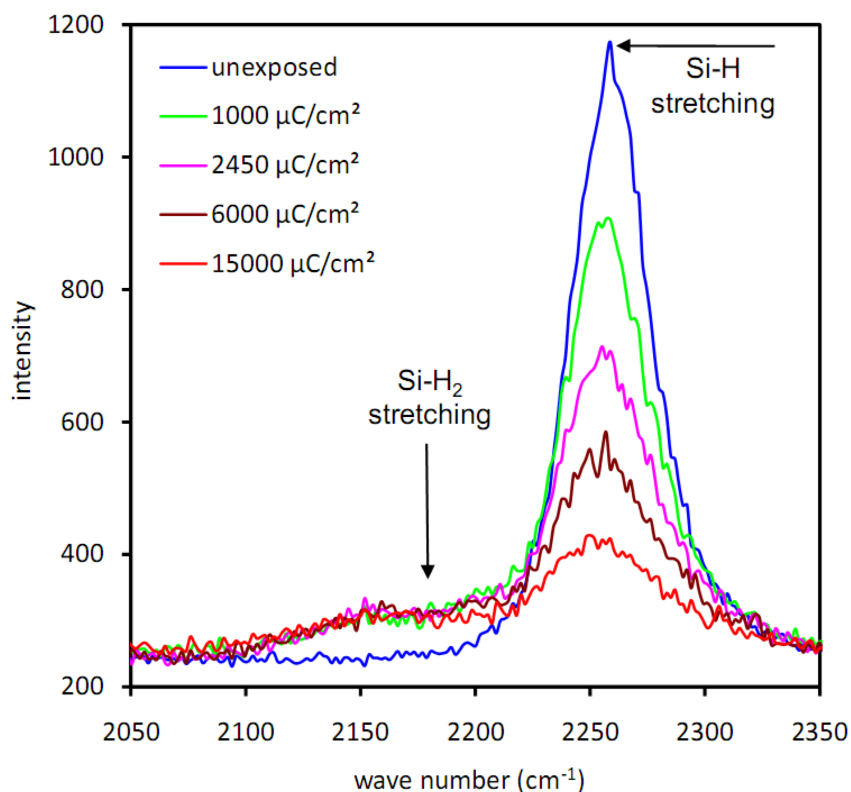

Figure 4: Raman spectra in the 2050-2350 cm^{-1} band for HSQ film on silicon, exposed to various doses of electron-beam radiation. The background signal of the silicon substrate was subtracted from all measurements. As in the thermal-curing case, the Si-H peak shrinks steadily with increasing electron dose. Peaks in the Si-H_2 region are broader and less well-resolved than in the thermal case, however, and also appear to saturate at a low electron dose, suggesting that the behavior in this regime may be more complex than in the thermal case.

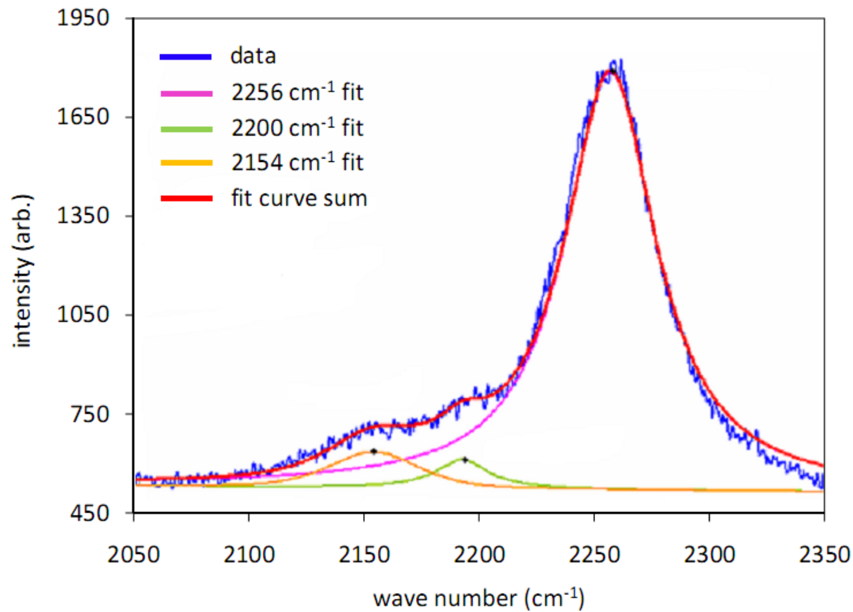

Figure 5: Raman spectra of the 2450 μC/cm^2 exposure in figure 4, fitted to three different Gaussian-Lorentzian peaks. The peak at 2194 cm^{-1} corresponds to the Si-H_2 vibration, while the peak at 2154 cm^{-1} corresponds to the Si-H_3 vibration. As the dose increases, the Si-H_2 peak decreases and the Si-H_3 peak increases, suggesting that increasing hydrogen redistribution in the resist during electron exposure will eventually progress to the point of creating volatile silane (SiH_4).

Electron-Beam-Induced Desorption (EBID)

To study the electron-induced reaction mechanisms in more detail, electron-beam-induced desorption (EBID) was performed on an unexposed HSQ film, and mass spectroscopy was used to monitor the products evolving from the film during beam exposure. EBID experiments were performed in a high-vacuum SEM[a] (base pressure ~ $2 \cdot 10^{-6}$ mbar) and in an ultra-high vacuum scanning Auger microscope[b] (base pressure ~ 10^{-9} mbar) using a quadrupole residual gas analyzer[c] with 5 and 10 keV beams incident on 180 nm HSQ films on Si substrates. The electron current density was ~ 0.05 μA/cm^2 in the SEM and ~ 4 μA/cm^2 in the Auger.

In a quadrupole mass spectrometer, gas molecules are ionized by electron bombardment, which can produce several ionized fragments from one parent molecule. The measured ion distribution, known as the cracking pattern, can vary depending on the type of mass spectrometer, and the tuning of the specific instrument. The absolute cracking pattern for silane by 50 eV electrons, determined by a Fourier-transform mass spectrometer, is SiH_4^+ 0%, SiH_3^+ 30%, SiH_2^+ 45%, SiH^+ 13%, and Si^+ 12%, with no detectible H^+ or H_2^+,[d] while another study[e] found a similar pattern with SiH_2^+ 40% and H^+ 5%. Raw data must be corrected for the silicon isotopic distribution (Si^{28} 92%, Si^{29} 4.7%, Si^{30} 3.1%). The mass resolution of quadrupole mass spectrometers is limited, so for example at mass 28, the CO^+, N_2^+ and Si^+ ions cannot be distinguished. The EBID experiments are complicated by the presence of background gasses, which limit the sensitivity to certain product species.

The primary species detected after exposure of the HSQ film to the electron beam were mass 2, corresponding to H_2, as well as masses 29, 30, and 31, which correspond to silane or SiH_x radicals. The mass spec used for these experiments was not sensitive to atomic H, and the background water pressure in the SEM EBID experiments was much larger than that of the detected SiH_x products. In the Auger EBID experiments, the water background was approximately an order of magnitude greater than the detected SiH_2 signal, and a barely detectable increase above background was observed during EBID, which suggests that the amount of water produced is not greater than the amount of SiH_x.

The absolute sensitivity of a quadrupole mass spectrometer varies with mass, and in particular the H_2 signal is a strong function of the instrument tuning. The observed SiH_x to H_2 ratios, which depend on instrument response and also the vacuum system pumping (80:1 in the SEM, and 800:1 in the Auger), do not give quantitative information on the relative amounts of SiH_x and H_2 generated during EBID.

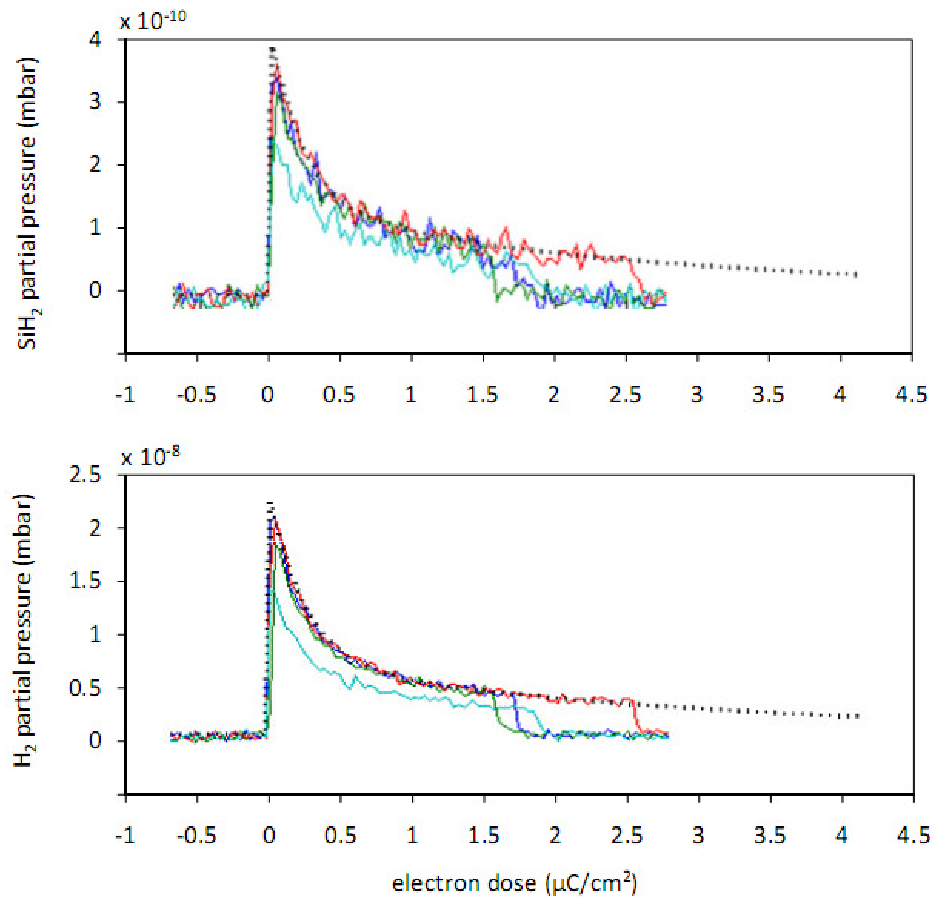

Figure 6: Electron-beam-induced desorption (EBID) data showing the partial pressures of H_2 and SiH_2 as a function of dose, obtained by exposing a 180-nm-thick HSQ film to a 5 KeV electron beam and recording the partial pressures of the various evolved products with a mass spectrometer. The ambient chamber pressure was ~ 2 x 10^{-6} mBar. When the beam is turned on, the partial pressures of both H_2 and SiH_2 immediately increased, and returned to baseline when the beam was switched off. The dose rate was ~ 0.05 uC/s. The presence of SiH_2 confirms the redistribution reaction suggested by the Raman results in the previous section. The solid lines are different experiments, and the broken line is a double-exponential fit to the data, with the same decay constants for H_2 and SiH_2.

Figure 6 shows the peaks which correspond to H_2 and SiH_2 ions, the dominant peaks measured during the process . The release of SiH_x products are consistent with the redistribution reaction proposed earlier; as

bonds are broken in the HSQ structure, H atoms will redistribute and bond to Si atoms to an increasing degree; the final result of this redistribution process is the production of SiH_4. or silane gas. The absolute peak ratios measured were 0.447, 1, 0.7 for masses 29, 31, and 32

There was a fixed H_2/SiH_2 ratio during EBID exposure, and the reaction rate with dose could be fit by a double exponential. The fast component had an exponential decay constant of 0.32 uC/cm^2 at 5 keV and 0.38 uC/cm^2 at 10 keV, and the slow component had a decay constant 12 times larger, or 3.8 and 4.5 uC/cm^2, respectively, with ~ 15% of the gas evolved during the fast process.

Discussion of HSQ reaction mechanisms

The Raman detection of SiH_2 and SiH_3 peaks in exposed HSQ, as well as the detection of evolved SiH_x during EBID indicates that a redistribution reaction is induced in HSQ by electron beam exposure. However, the release of molecular hydrogen with a similar does dependence to silane during EBID suggests that other reactions are occurring as well Siew *et al.* summarized several reactions that occur in the thermal curing of HSQ.[23] The redistribution reaction

$$2HSiO_{3/2} \rightarrow H_2SiO_{2/2} + SiO_{4/2} \quad (4)$$

results in silane evolution as multiple hydrogens are added to the same silicon site. H_2 evolution is a result of the reaction schemes below:

$$2H_2SiO \rightarrow 2H_2 + =OSi\text{-}SiO= \quad (5)$$

$$2H_2SiO \rightarrow SiH_4 + SiO_{4/2} \quad (6)$$

.

At higher temperatures (above 400 C), H_2 can evolve due to the dehydrogenation of Si-H such that.

$$2HSiO_{3/2} \rightarrow H_2 + =OSi\text{-}SiO= \qquad (7)$$

In electron-beam-exposed material, the electron energies are very high compared to thermal energies; hence, there should be enough energy to initiate any of these reactions. The release of H_2 along with SiH_x products in the EBID data indicates that the Raman Si-H peak reduction with increasing electron exposure cannot solely be attributed to the redistribution reaction. The substantial H_2 release is consistent with Albrecht and Blanchette's thermal desorption data from HSQ above 410°C, which showed H_2 being produced at two orders of magnitude higher than SiH_4 and was attributed to reaction mechanism (7). Furthermore, we have used Auger spectroscopy to show that continued exposure of the material in vacuum (at doses much higher than normally used for electron beam lithography) results in a silicon-rich oxide. The EBID data also calls into question the role water in the film plays in the e-beam induced crosslinking mechanism suggested by Namatsu *et al.*[1] Water is detected at a pressure two orders of magnitude below H_2 during EBID, barely above the background signal. Namatsu's reaction would produce 1 H_20 for every two H_2 produced. This is not consistent with the ratio of hydrogen to water that we detect. Even if a water reaction product was consumed in the reaction via reaction scheme (2), water would be expected to escape at the edges of the reaction front and be detected at higher levels in the EBID. However, because we have observed that exposed, undeveloped films that showed a thickness reduction after exposure[17] would recover their original thickness after a few weeks (suggesting absorption of ambient H_2O or O_2 by the film), we cannot rule out that reactions (2) and (3) occur after removal from the lithography system.

In terms of the observed area-dependent exposure dose for HSQ,[15,17] dehydrogenation of silicon may be playing an important role. In radiation exposed polydimethyl silsesquioxane films, hydrogen radicals diffuse considerable distances before reacting.[24] We suspect HSQ would behave similarly and allow hydrogen radicals to diffuse through the film and extract hydrogen in unexposed areas. This can leave reactive silicon radicals behind, facilitating the formation of Si-Si bonds during subsequent exposure. Alternatively, Si-O-Si bonds can form when hydrogen is extracted from an Si-OH bond which can subsequently react with neighboring silicon radials. Work by Castor et. al. suggest that a primary peak observed in NEXAFS in HSQ at the oxygen edge is due to Si-OH.[25]This peak decreases during x-ray exposure and in the areas surrounding the exposure. However, there could be several potential pathways to this area-dependent exposure and more study is needed.

Conclusion and Further Work

Investigations with Raman spectroscopy and EBID have revealed the behavior of HSQ when exposed to radiation (such as high energy electron introduced during electron beam lithography) to be more complex than previously suggested.[1] Raman and EBID studies show that electron beam exposed HSQ undergoes a redistribution reaction taking place that cross-links the system via oxygen bridges between HSQ molecules and, in the process, generates silane (SiH_4). This behavior is supported by the appearance of $Si\text{-}H_2$ and $Si\text{-}H_3$ vibration modes when Raman spectroscopy is performed on exposed resist, as well as the production of SiH_x products during EBID. Additionally, hydrogen gas evolves during EBID at a level two order of magnitude, which suggests additional exposure mechanisms, such as the formation of Si-Si bonds to form a silicon rich oxide. Raman studies of HSQ on substrates which give good signal over substrate background for detection of the Si-Si peaks will help clarify this additional exposure pathway. Furthermore, additional work is needed to understand the instabilities and area-dependent exposure

mechanisms in HSQ. As HSQ is becoming increasingly popular as a high-resolution electron resist, these topics hold practical importance and certainly warrant further study.

Acknowledgements

The authors would like to thank Adam Schwartzberg for useful discussions on Raman Spectra and Prof. Thomas Klassen, head of the student exchange program at Helmut-Schmidt University. This work was performed at the Molecular Foundry, Lawrence Berkeley National Laboratory, and was supported by the Office of Science, Office of Basic Energy Sciences, of the U.S. Department of Energy under Contract No. DE-AC02—05CH11231 . A. S. was supported by the student exchange program at Helmut-Schmidt University. B. C. was supported by Vistec.

References

1. H. Namatsu, Y. Takahashi, K. Yamazaki, T. Yamaguchi, M. Nagase, and K. Kurihara, J. Vac. Sci. Technol. B 16, 69 (1998).
2. I. Junarsa, M. P. Stoykovich, and P. F. Nealey, J. Vac. Sci. Technol. B 23, 138 (2005).
3. S. Matsui, Y. Igaku, H. Ishigaki, J. Fujita, M. Ishida, Y. Ochiai, H. Namatsu, and M. Komuro, J. Vac. Sci. Technol. B 21, 688 (2003).
4. K. Nakamatsu, K. Watanabe, K. Tone, T. Katase, W. Hattori, Y. Ochiai, T. Matsuo, M. Sasago, H. Namatsu, M. Komuro, and S. Matsui, Jpn. J. Appl. Phys 43, 4040 (2004).
5. K. A. Lister, B. G. Casey, P. S. Dobson, S. Thoms, D. S. Macintyre, C. D. W. Wilkinson, and J. M. R. Weaver, Microelectron. Eng. 73-74, 319 (2004).
6. J. K. W. Yang and K. K. Berggren, J. Vac. Sci. Technol. B 25, 2025 (2007).
7. F. C. M. J. M. van Delft and F. G. Holthuysen, Microelectron. Eng. 46, 369 (1999).

[8] F. J. Feher, R. Terroba, R. Jin, K. O. Wyndham, S. Lucke, R. Brutchey, and F. Nguyen, Polym. Mater. Sci. Eng. 82, 301 (2000).

[9] G. Li, L. Wang, H. Ni, and C. U. Pittman, J. Inorg. Organomet. Polym. 11, 123 (2001).

[10] M. G. Albrecht and C. Blanchette, J. Electrochem. Soc. 145, 4019 (1998).

[11] K. Maex, M. R. Baklanov, D. Shamiryan, and F. Iacopi, J. Appl. Phys. 93, 8793 (2003).

[12] H. Namatsu, T. Yamaguchi, M. Nagase, K. Yamazaki, and K. Kurihara, Microelectron. Eng. 41-42, 331 (1998).

[13] G. M. Schmid, L. E. Carpenter, and J. A. Liddle, J. Vac. Sci. Technol. B 22, 3497 (2004).

[14] W. Henschel, Y. M. Georgiev, and H. Kurz, J. Vac. Sci. Technol. B 21, 2018 (2003).

[15] J. A. Liddle, F. Salmassi, P. P. Naulleau, and E. M. Gullikson, J. Vac. Sci. Technol. B 21, 2980 (2003).

[16] F. C. M. J. M. van Delft, J. P. Weterings, A. K. van Langen-Suurling, and H. Romijn, J. Vac. Sci. Technol. B 18, 3419 (2000).

[17] D. L. Olynick, J. A. Liddle, A. V. Tivanski, and M. K. Gilles, J. Vac. Sci. Technol. B 24, 3048 (2006).

[18] J. L. Koenig and J. P. Bobiak, Macromol. Mater. Eng. 292, 801 (2007).

[19] L. Muntean, R. Planques, A. L. D. Kilcoyne, S. R. Leone, M. K. Gilles, and W. D. Hinsberg, J. Vac. Sci. Technol. B 23, 1630 (2005).

[20] P. J. Schuck, D. P. Fromm, A. Sundaramurthy, G. S. Kino, and W. E. Moerner, Phys. Rev. Lett. 94 (2005).

[21] P. Bornhauser and G. Calzaferri, J. Phys. Chem. 100, 1996 (1996).

[22] M. J. Loboda, C. M. Grove, and R. F. Schneider, J. Electrochem. Soc. 145, 2861 (1998).

[23] Y. K. Siew, G. Sarkar, X. Hu, J. Hui, A. See, and C. T. Chua, J. Electrochem. Soc. 147, 335 (2000).

[24] A. Charlesby and P. G. Garratt, Proc. Royal Soc. London A 273, 117 (1963).

[25] A. G. Caster, S. Kowarik, A. M. Schwartzberg, A. V. Tivanski, M. K. Gilles, and S. R. Leone, in preparation (2009).

---

[a] Zeiss Gemini Supra VP
[b] Physical Electronics PHI 660
[c] Stanford Research Instruments
[d] Peter Haaland, Chem Phys Lett 170 146 (1990).
[e] R. Basner, M. Schmidt, V. Tarnovsky, K. Becker and H. Deutsch, Int. J. Mass. Spec. Ion Proc. 171 83 (1997).